ELSEVIER

Organosilane and lignosulfonate as innovative stabilization techniques for crushed rocks used in road unbound layers

Diego Maria Barbieri[a,*], Inge Hoff[a], Mai Britt Engeness Mørk[b]

[a] Norwegian University of Science and Technology, Department of Civil and Environmental Engineering, Høgskoleringen 7A, Trondheim 7491, Trøndelag, Norway
[b] Norwegian University of Science and Technology, Department of Geosciences and Petroleum, Sem Sælandsvei 1, Trondheim 7491, Trøndelag, Norway

A B S T R A C T

The tunnelling operations connected to the construction of the new Norwegian E39 highway generate a considerable amount of blasted rocks. The local use of these rocks as construction materials in the unbound layers of the highway represents a sustainable cost-benefit application. Two non-traditional stabilizing additives improve the mechanical properties of the aggregates not fulfilling the code strength requirements: one is based on organosilane, the other one is based on lignosulfonate. Laboratory investigations (thin-section microscopy, X-ray crystallography, X-ray fluorescence, repeated load triaxial test) characterize the rock materials and the effectiveness of the additives. The research further investigates the performance of three typical road base layer sections specifically built according to real practice and treated with water (no treatment), organosilane and lignosulfonate, respectively. They are exposed to climatic conditions only; no surface courses and no trafficking actions are applied. The developments of the layers' stiffness and deformation are assessed by means of light weight deflectometer and dynamic cone penetrometer. The time span covered by the investigation is one year, both in the laboratory and in the field. The stabilizing additives can enhance the mechanical properties of the crushed rocks.

Introduction

Tunnelling operations and generation of crushed rocks

Norwegian Public Roads Administration (NPRA) is currently running the "Ferry-free coastal highway route E39" project, which improves the viability along the southwestern Norwegian coast for a total length of about 1100 km from Trondheim to Kristiansand [52]. The project has a remarkable national relevance as the industries located along the route generate about half of Norway's traditional export [26]. The extended tunnelling systems will produce a very large quantity of blasted rocks; they could potentially be used as local construction materials, namely aggregates, in the road unbound layers, thus reducing the consumption of natural resources and entailing major advantages from several points of view [31,57,59]. The transport distance of the blasted materials should be within 20–30 km to represent a competitive solution compared to the purchase of quarry virgin aggregates [8,48]. Previous experience regarding the usability strategies of tunnel excavation materials highlighted the importance for construction management and economics [11,33,45,58]. Furthermore, the concern about environmentally-friendly and sustainable solutions is

becoming more and more relevant in Norway, as it pledges to reach climate neutrality by 2030 [69].

The Norwegian pavement design manual N200 [51,54] sets certain requirements regarding the properties of the unbound granular materials (UGMs) to be used in the unbound layers not to encounter premature damage [4]: grain shape [14], flakiness index value [15], Los Angeles (LA) value [17] and micro-Deval (MDE) value [16].

A previous research [5] characterised the bedrock geology which is spread along the highway alignment. Igneous rocks and supracrustal rocks of Precambrian ages (1700–900·106 years) represent the most widespread geology. They mainly comprise granite, granodiorite and granitic to dioritic gneiss; which are variably influenced by metamorphism and deformation related to the Caledonian orogeny. Some rocks ("strong" aggregates) fulfil the requirements specified in the pavement design manual, while other rocks ("weak" aggregates) do not.

Crushed rocks stabilization techniques

Currently there are several stabilization methods available for roadway unbound courses, e.g. cement, bitumen, lime, fly ash, gypsum [7,30,41,47,55,62,64]. Two non-traditional additives showed
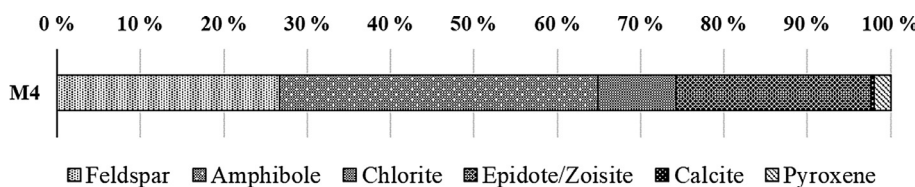
Fig. 1. Bulk mineralogy of the investigated crushed rocks.

promising laboratory results as they enhanced the resilient modulus and the resistance to permanent deformation of the "weak" rocks [6]; one additive was based on organosylane, here referred to also as polymer-based (P) agent, and the other additive was based on lignosulfonate, here referred to also as lignin-based (L) agent. This research expanded the previous investigation by means of further tests both in the laboratory and in the field. The goal is to assess the effectiveness of the additives more thoroughly and draw suggestion for their practical use.

The polymer-based (P) agent is a non-leachable and UV- & heat-stable product. This additive derived from nanoscale technology is made of two components (here referred to as C1 and C2), which chemically convert the water absorbing silanol groups presented on the silicate-containing surface of the rocks to a 4–6 nm layer of hydrophobic alkyl siloxane. The siloxane ($=Si-O-Si=$) linkage is a strong chemical covalent polar bond and results in near permanent modifications. The technology imparts water resistance, better lubrication for compaction and bonding action at ambient temperature [39,56]. The additive modifies the rocks' surfaces and mechanical improvements can be measured at a macroscale level [60,65,66]. The existing limited experience shows favourable results and solely refers to silty and clayey soils tested in the laboratory [23,70] and in the field [42]; therefore, the research experimented with a new application context related to stabilization of crushed rocks. The safety data sheets of components C1 and C2 did not report any environmental hazard: leakage tests were performed [10,24] and Dissolved Organic Carbon (DOC) parameter was assessed, the degradation is environmentally acceptable.

The lignin-based (L) agent is a renewable product of the pulp and paper industry. It is an organic polymer that consists of both hydrophilic and hydrophobic groups, it is non-corrosive, non-toxic and water-soluble [1,61]. Previous experiments investigating the strength and density modification of unpaved road using lignosulfonate showed promising outcomes for silty and clayey soils both in the laboratory [1,22,61,68,75] and in the field [37,53,76]. As in the case of the polymer-based additive, the application of the lignin-based additive to crushed rocks could result in a wider acceptance of this stabilizing technology.

The research was carried out both in the laboratory and in the field. Laboratory tests comprised geological characterization by means of thin-section microscopy, X-Ray Diffractometry (XRD), X-Ray Fluorescence (XRF) and mechanical characterization by means of Repeated Load Triaxial Test (RLTT) [18]. The investigation in the field focused on three typical base road sections built according to real Norwegian construction practice and added with water (no treatment), polymer-based additive and lignin-based additive, respectively. The three road sections were exposed to climatic conditions only; no surface courses, i.e. bituminous layer, and no trafficking actions were applied. The developments of the layers' stiffness and deformation was assessed by means of Light Weight Deflectometer (LWD) [3] and Dynamic Cone Penetrometer (DCP) [2]. The time span covered by the investigation was one year, both in the laboratory and in the field. The field test accomplished in this research adopted aggregates that do fulfil standard code requirements. Arranging the field test using a "weak" material was not possible for practical and economic reasons, since it was not feasible to find enough quantities of "weak" aggregates from quarries. This did not hinder the general purpose of the research, namely, to investigate whether the use of the additives can improve the mechanical properties of a given type of crushed rocks. Therefore, benefits may even be greater for poorer rock aggregates.

Methodology

Geological characterization of the crushed rocks

The aggregates used in the research came from Vassfjellet, the area is close to Trondheim (Trøndelag, Norway) and has several quarries; they are particularly rich in greenschist and gabbro. The Vassfjellet greenstone is composed of meta-gabbro, meta-dolerite and meta-basalt [32,74]. The investigated crushed rock material is here also referred to as material M4 (after having tested materials M1, M2 and M3 in [6]).

Thin section microscopy

Thin-section microscopy images of selected rock samples showed mineralogy and grain sizes. The igneous texture with plagioclase laths was visible in cross-polarized light. Metamorphic reactions caused replacement of igneous pyroxene by amphibole, and growth of epidote/zoisite within the igneous plagioclase laths. M4 samples also included small amounts of fine-grained metagabbro/meta-dolerite varieties; the rock could be classified as gabbro/metagabbro.

XRD and XRF analyses

Batches of material M4 were prepared for XRD diffractometer analyses to identify the main mineralogical compositions according to Rietveld mineral quantification. Samples were crushed, split, milled to 10 μm and analysed as powder preparate in the XRD diffractometer. Fig. 1 displays semi-quantitative weight proportions of the most abundant minerals.

Feldspar, amphibole and epidote/zoisite were the predominant minerals. Compared to M1, M2 and M3 compositions [5], the M4 mineralogy deviated by a higher content of mafic (iron-bearing) silicate minerals and absence of quartz. X-Ray Fluorescence (XRF) bulk chemical analysis displayed the chemical composition of the rocks as a percentage of the total mass. Samples were grinded and ignited to 550 °C. Silicon was the major component [32].

Mechanical characterization of the crushed rocks

Standard tests characterization

The pavement design manual N200 [51,54] sets requirements for employing crushed rocks. The aggregates can be used in the road base layer as paved crushed rocks and in the road subbase layer as unsorted crushed rocks if the Los-Angeles standard test (LA value) and micro-Deval standard test (MDE value) are fulfilled. The LA limit values are 30 and 35 for base layer and subbase layer respectively, the MDE limit value is 15 for both. The chosen material M4 did fulfil the code requirements (i.e. it is a "strong" aggregate), since the Los-Angeles and micro-Deval values were 18.2 and 14.2 respectively.

The grain size distribution curve used in the investigation both in the laboratory and in the field is displayed in Fig. 2. The grain sizes were smaller than 32 mm. The gradation attained in the field after the mixing and compaction operations was evaluated as well: since the two distribution curves were very close (as expected due to the good LA value), Fig. 2 only displays one curve. Fig. 2 also shows the range of particle sizes [12]. Optimum Moisture Content (OMC) was assessed for the investigated UGMs [19], it was equal to 5% for bulk density approximately equal to 2.5 t/m^3.
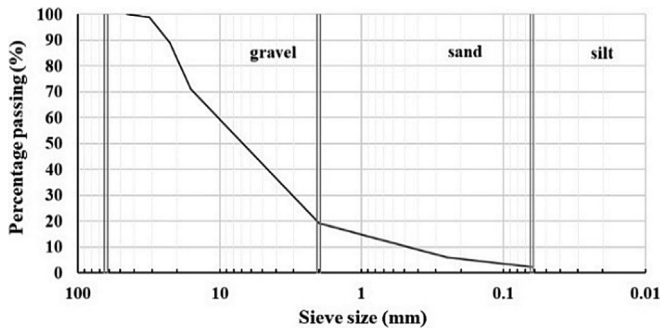
Fig. 2. Grain size distribution curve (base layer) used in laboratory and field tests.

Repeated load triaxial test

Repeated Load Triaxial Test (RLTT) gives a comprehensive insight into material properties by assessing the stiffness and the resistance to permanent deformation. The UGM's behaviour is connected to the following parameters: stress level, moisture content, dry density, grading and mineralogy, etc. [43,44,67,72].

The preparation of the specimen was carried out based on the following procedure. Firstly, 7300 g of dry material were prepared according to the grading curve reported in Fig. 2. Consequently, the desired amount of water, and additive if needed by the test, was added. The mixture was divided into four parts and rested in as many impermeable bags for 24 h. The operator then compacted the four layers inside a steel mould; the bulk density and dry density were assessed [19]. A Kango 950X vibratory hammer (total weight 35 kg, frequency 25–60 Hz, amplitude 5 mm) was used to compact the layers inside the mould, the compaction time was 30 s per layer. Finally, the sample was covered by latex membranes and end-platens, sealed by rubber O-rings and hose clamps. All the samples had a diameter of 150 mm and the final height varied between 170 and 190 mm. The sample height differed from the indication given by the code, where the height is recommended to be twice the diameter of the sample [18]. Research regarding the influence of the height to diameter ratio with respect both to resilient modulus and permanent deformations demonstrated that samples with a ratio ranging from 1:1 to 1.5:1 show little differences. Teflon foils and silicon oil were used for lubrication to secure low friction against the end-platens [25].

Samples with additives were conditioned carefully prior to testing in order to reach approximately the same water content, thus enabling a clearer comparison of results. The lignin-based additive needs to dry to attach the material particles and become effective; the polymer-based additive is effective even with higher water content [6].

The polymer-based additive was mixed at OMC. The following proportion was used: 18 g C1 + 18 g C2 for 365 g of water, this was already found to be a reasonable amount [6]. The dosage was higher than the recommended use for silty and clayey materials. Each RLTT sample was firstly conditioned at 65 °C for 24 h and then at 22 °C (room temperature) for 24 h before testing.

The lignin-based additive was mixed at OMC; the percentage added to the crushed rocks was 1.5% in mass. The dosage was similar to the recommended use for silty and clayey materials. Lignosulfonate needs a curing time to dry in order to become effective and attach properly to the material particles [22,61,68]. Each RLTT sample was firstly conditioned at 65 °C for 48 h and then at 22 °C (room temperature) for 24 h before testing.

RLTT apparatus exerts a uniform confining pressure in all the directions (σ_3, triaxial or confining stress) and an additional vertical dynamic stress (σ_d, deviatoric stress), which is applied according to the chosen sinusoidal pattern and stepwise increases with different levels of σ_3. The RLTT apparatus performed the multi-stage low stress level (MS LSL) loading procedure: five sequences are associated with five different σ_3 values (σ_3 = 20, 45, 70, 100, 150 kPa). In addition, six steps are associated to six given σ_d values and form each sequence [18]. The five loading sequences and the respective loading increments can be displayed according to bulk stress θ ($\theta = \sigma_1 + \sigma_2 + \sigma_3$ the sum of the principal stresses) and σ_d. Therefore, a RLTT comprises 30 loading steps consisting of 10 000 load pulses at 10 Hz frequency. A loading sequence is interrupted if the axial permanent deformation reaches 0.5%. Three Linear Variable Differential Transducers (LVDTs) measured the axial deformations, and again, three other LVDTs measured the radial deformation. Replicate specimens (two samples) were used for each RLTT and average results are displayed in the results section. The resilient modulus M_R associated with a change in the dynamic deviatoric stress σ_d^{dyn} and constant σ_3 is defined as follows

$$M_R = \frac{\Delta \sigma_d^{dyn}}{\varepsilon_a^{el}} \tag{1}$$

where ε_a^{el} is the axial resilient strain. Several non-linear relationships are proposed to describe M_R with reference to bulk stress θ [43]. The following k-θ relationship was adopted [34]

$$M_R = k_1 \sigma_a \left(\frac{\theta}{\sigma_a} \right)^{k_2}, \tag{2}$$

where σ_a is a reference pressure (100 kPa) and k_1, k_2 are regression parameters. The relationship enabled a clear comparison in two-dimensional plots between the materials' performances.

The resistance to permanent deformation was investigated through the Coulomb approach [38]. The Coulomb criterion relates the mobilized shear strength to the development of permanent deformations and the maximum shear strength to incremental failure. The mobilized angle of friction φ_{mob} and the angle of friction at incremental failure φ_{max} respectively express the degree of mobilized shear strength and the maximum shear strength. The angle of friction and the angle of friction at incremental failure identify three different ranges of material behaviour: elastic, elasto-plastic and failure. The strain rate $\dot{\varepsilon}$ is a measure of the speed of the permanent deformation; this parameter refers to the development of permanent deformation per cycle. Table 1 defines the two boundary lines between the three ranges: each load step is categorised considering the average strain rate for the cycles from 5 000 to 10 000 [6,38].

The equations defining the elastic limit line and incremental failure line are respectively

$$\sigma_d = \frac{2\sin\varphi_{mob}(\sigma_3 + a)}{1 - \sin\varphi_{mob}} \tag{3}$$

$$\sigma_d = \frac{2\sin\varphi_{max}(\sigma_3 + a)}{1 - \sin\varphi_{max}}; \tag{4}$$

a regression analysis was used to assess the boundary lines. As a simplification, the apparent attraction a was assumed to be 20 kPa for all the samples [72].

The RLTTs were performed in May 2018. The specimens were successively placed in plastic boxes and stored outside in the laboratory backyard exposed to the natural climatic variations (Fig. 3a). The boxes were carefully closed to prevent the entrance of sunlight and precipitation; otherwise, the sunlight could destroy the latex membranes surrounding the aggregates. Fig. 3b displays a top view of the samples, highlighting the different surface appearance. The specimens were

Table 1
Permanent strain rate values defining the material range boundary lines.

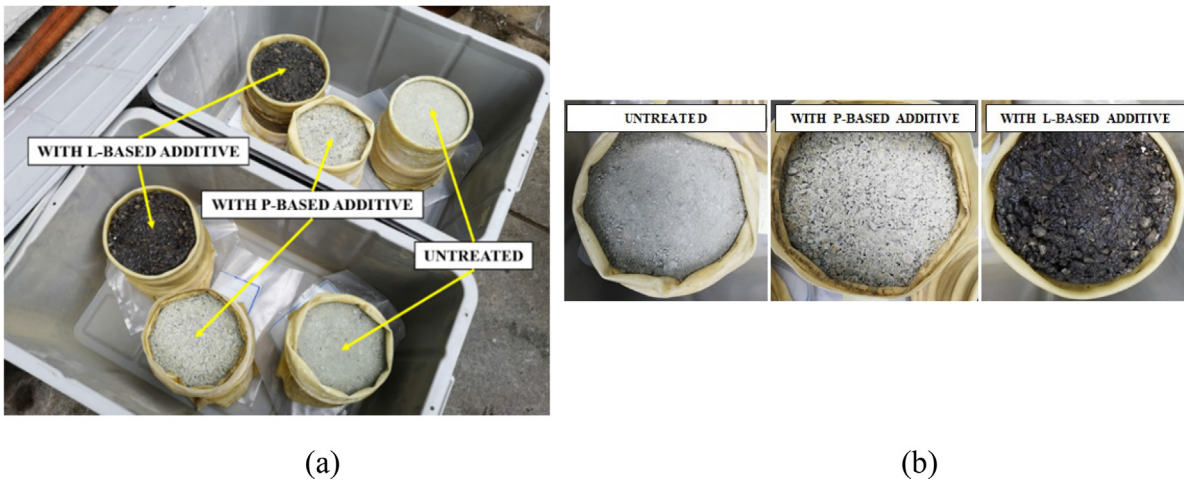| Permanent strain rate	Range
$\dot{\varepsilon} < 2.5 \cdot 10^{-8}$	Elastic zone
$2.5 \cdot 10^{-8} < \dot{\varepsilon} < 1.0 \cdot 10^{-7}$	Elasto-plastic zone
$\dot{\varepsilon} > 1.0 \cdot 10^{-7}$	Plastic (incremental failure) zone

(a)

(b)

Fig. 3. Outdoor storage of the RLTT specimens tested in May 2018 and May 2019 (a). Top view of the samples (b).

(a)

(b)

(c)

(d)

(e)

(f)

Fig. 4. Construction of the first 15-cm course of the base layer: laying of the material (a), spreading water at L0 (b), spreading polymer-based additive at L1 (c), spreading lignin-based additive at L2 (d), mixing (e) and compacting (f).

Table 2
Quantity of water and additives used in each location with 15-cm thick layer.

Location	Water (kg)	P-based additive (kg)		L-based additive (kg)
		component C1	component C2	
L0	500	0	0	0
L1	500	26	26	0
L2	500	0	0	150

newly investigated by means of RLTTs in May 2019 to assess the variation in the mechanical properties after one year. Average, minimum, maximum temperature were daily recorded in the two closest weather stations: Risvollan station and Voll station [50], both are approximately located 2 km away from the laboratory. The values of the mentioned parameters were obtained based on the distance weighting method [71].

Field Test

Construction procedure

The field test was located in a large area available inside a quarry in Vassfjellet. Three base layer sections were built using the grain size distribution curve already displayed in Fig. 2. They corresponded to three locations which underwent different treatments: just water/untreated (location L0), polymer-based additive (location L1), lignin-based additive (location L2); each section was approximately 0.3 m thick before compaction, 3.5 m wide and 10 m long. As a first step, the existing rocky subgrade was covered by a homogeneous capping layer made of aggregates with fraction 0/8 mm, the thickness was approximately 50 cm. Afterwards, a roller compactor compacted the capping layer uniformly. Bomag BW 177 D-4 was the single steel drum roller used for this purpose. Its weight is 7.5 t, the drum axle load is 4.2 t, the wheel axle load is 3.3 t, the static linear load is 24.9 kg/cm and the working width is 1.7 m; the roller compactor accomplished seven
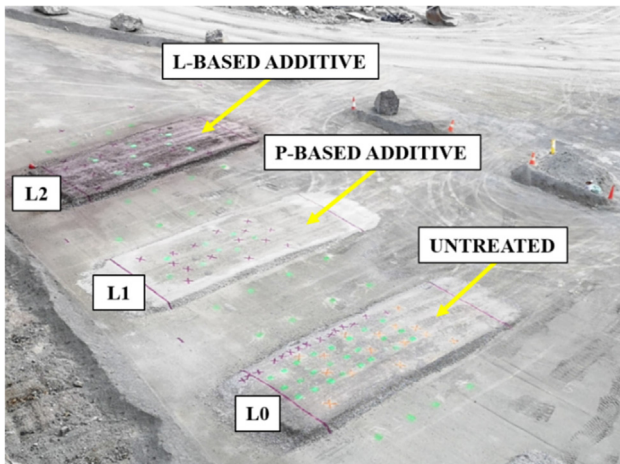
Fig. 5. Construction completion of the road base sections: with water (L0), with polymer-based additive (L1), with lignin-based additive (L2).

passages as specified in the manual code [54]. Since the zone of influence of the LWD is between 1.5 and 2 times the 30-cm diameter of the LWD plate [27], the attained thickness of the capping layer removed the influence of the inhomogeneous rocky subgrade on the LWD measurements.

The 30-cm thick base layer was achieved by laying two 15-cm thick layers successively; in this way the construction operations could ensure a proper homogeneous mixture between the crushed rocks and the additives spread on the top. Each 15-cm course corresponded to 10 tons of crushed rocks employed in each location (Fig. 4a). Water and additives were transported to the field thanks to Intermediate Bulk Containers (IBCs); before pumping out their contents, operators used a mixing drill to attain more homogeneous solutions. Each location was treated carefully applying the same proportions already tested in the laboratory as reported in Section 'Repeated load triaxial test' (Fig. 4b–d), Table 2 reports the quantity of the admixtures used in the field at this stage. Afterwards, a light recycler machine operated achieving two passages (Fig. 4e). The teeth of the shifting rotor gently blended the aggregates with the water and additives spread on the top of the layers down to a depth of 15 cm. Finally, the roller compactor Bomag BW 177 D-4 compacted each location with five passages as specified in the manual code [54](Fig. 4f). These construction operations were the same as used in Norway to build a base layer of a real road.

Successively, the second 15-cm thick course completing the final 30-cm thick base layer was placed and underwent the same procedure; therefore, the final amount of the admixtures used in the field was twice as displayed in Table 2. Due to the compaction operations, the final achieved thickness decreased from 30 cm to approximately 17 cm. The construction processes did not significantly alter the grain size

distribution curve, as earlier discussed in Section 'Standard tests characterization'. Compared to untreated location L0, the price uplift connected to the use of the additives was of 16% for location L1 and 14% for location L2. Fig. 5 shows the completion of the three road base sections.

Measurement procedures

The main device adopted in the field to assess the additives' effectiveness was the Light Weight Deflectometer (LWD). LWD is a single-person-use portable device used for the determination of bearing capacity and compaction quality of soils and unbound materials [3,35–36].The LWD employs the same technology of the Falling Weight Deflectometer (FWD) equipment: the major differences are the reduced load pulse duration and reduced maximum applied force [29,46]. The LWD used a single sensor: the loading mechanism generates a defined impulsive load and a geophone is the deflection transducer. After completion of three measurements, the average settlement S_m and the elastic modulus E_{LWD} are evaluated [9,73]. In order to assess the effectiveness of the additives, the goal of the research laid more weight on comparing the LWD results for the three investigated locations than in obtaining absolute values for each of them.

Another instrument used to evaluate the additives' performances was the Dynamic Cone Penetrometer (DCP), the device provided a measure of the material's in situ resistance to penetration. The test was performed by driving a metal cone into the granular material with a 8 kg weight dropped from a distance of 575 mm [2]. Test results might be correlated to other properties, e.g. resilient modulus and bearing capacity [20,21,63]. DCP device was used in the research as a further practical technique to assess the additives' performances in addition to LWD.

LWD measurements were taken on a daily basis for 50 days starting from 48 h after construction (May and June 2018). In case of precipitation, the measurements were carried out after it had stopped raining. Furthermore, LWD measurements were performed from day 110 to day 115 (September 2018) and from day 365 to day 370 (May 2019) after construction. The measuring operations comprising DCP took place during day 115 and day 370. Therefore, the time span covered by the field investigation was one year. Average, minimum, maximum temperature and precipitation were daily recorded in the two closest weather stations: Skjetlein station and Saupstad station [50], both of them were approximately located 5 km away from the test site. The values of the mentioned parameters were obtained based on the distance weighting method [71].

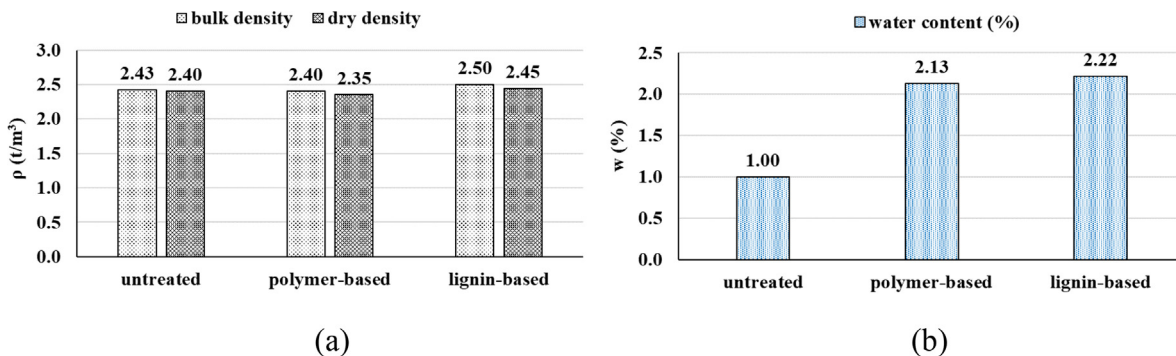There were 15 spots to accomplish LWD and DCP measurements in each location.

(a)

(b)

Fig. 6. Bulk density, dry density (a) and water content (b), for the specimens tested in the laboratory in May 2018.
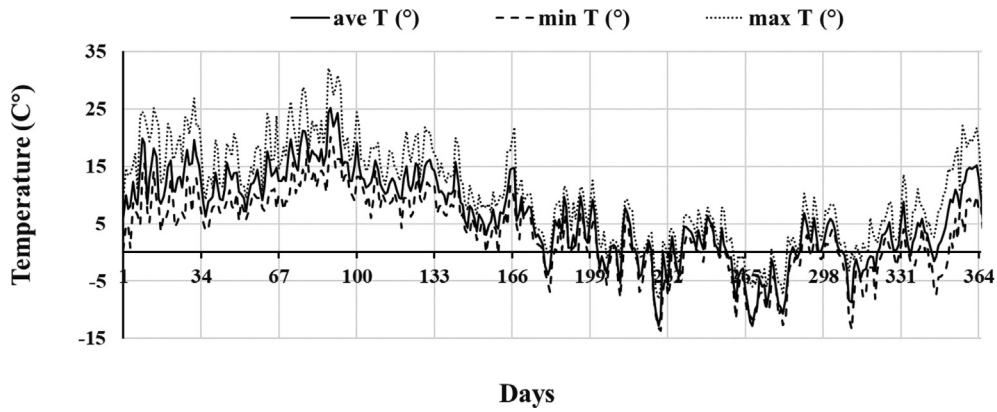
Fig. 7. Climatic conditions for the 1-year storage of laboratory samples: average, minimum and maximum temperature.
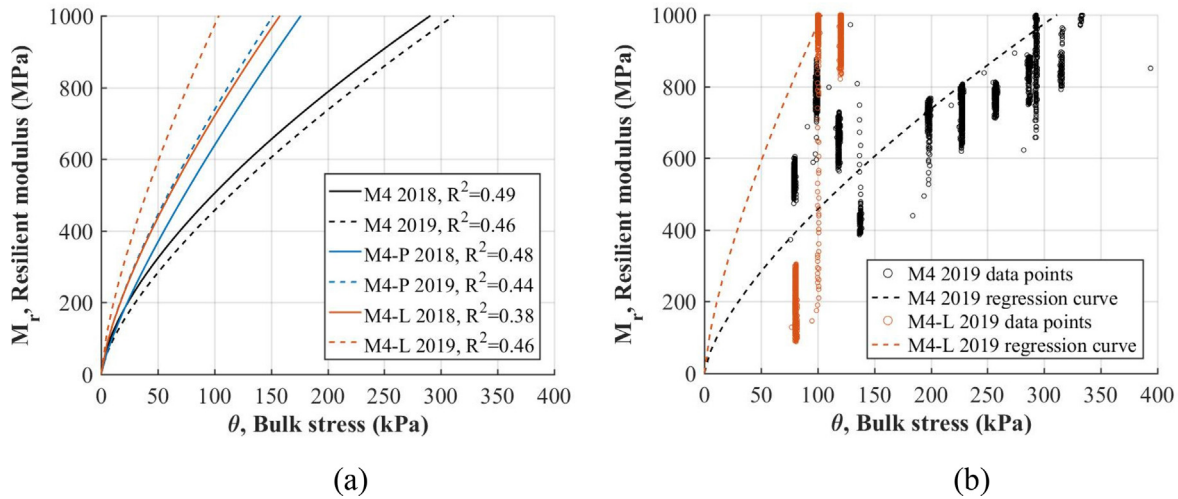

(a)

(b)

Fig. 8. Resilient modulus of untreated material (M4), with polymer-based additive (M4-P) and with lignin-based additive (M4-L), tested in May 2018 and May 2019 (a). Data points and corresponding regression curves for M4 2019 and M4-L 2019 (b).
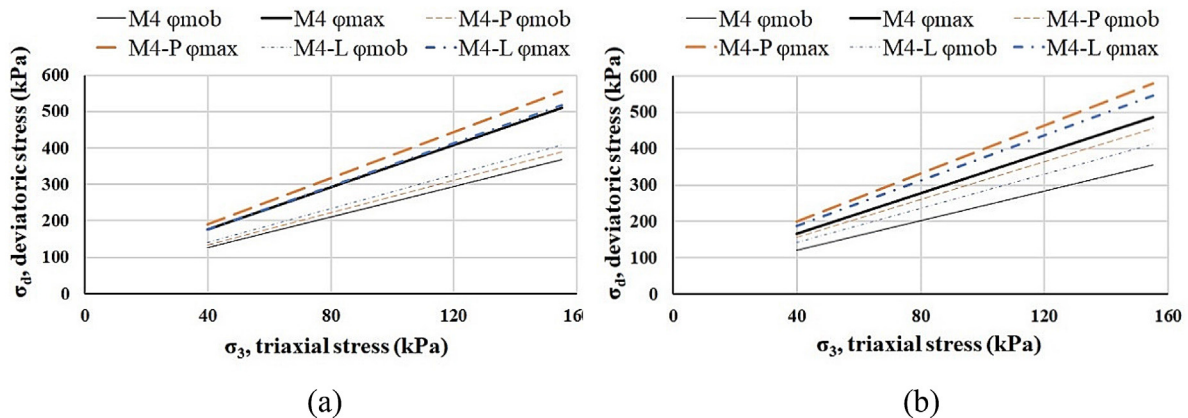

(a)

(b)

Fig. 9. Mobilized angle of friction φ_{mob} and angle of friction at incremental failure φ_{max} of the investigated specimens in May 2018 (a) and May 2019 (b).

Test results and discussion

Repeated load triaxial test

Fig. 6a illustrates the bulk and dry density of the specimens tested in May 2018. The measured water contents w after the curing process were close to $w = 2\%$ for the treated materials, this was higher than $w = 1\%$ used for the untreated material (Fig. 6b). This enabled a cautious comparison since M_R gradually reduces as w increases [28].

Resilient modulus k-θ relationships were evaluated (Eq. (2)) through data regression. As previously described in Section 'Repeated load triaxial test', the specimens were stored outdoor for one year and were exposed to the temperature variations reported in Fig. 7; the samples would have come out of a thaw period. Fig. 8a displays the results with solid lines, both polymer-based and lignin-based additive accomplished enhanced (stiffer) resilient curves; this result agreed with that already found in the previous laboratory experiences investigating other types of crushed rocks [6]. The polymer-based additive
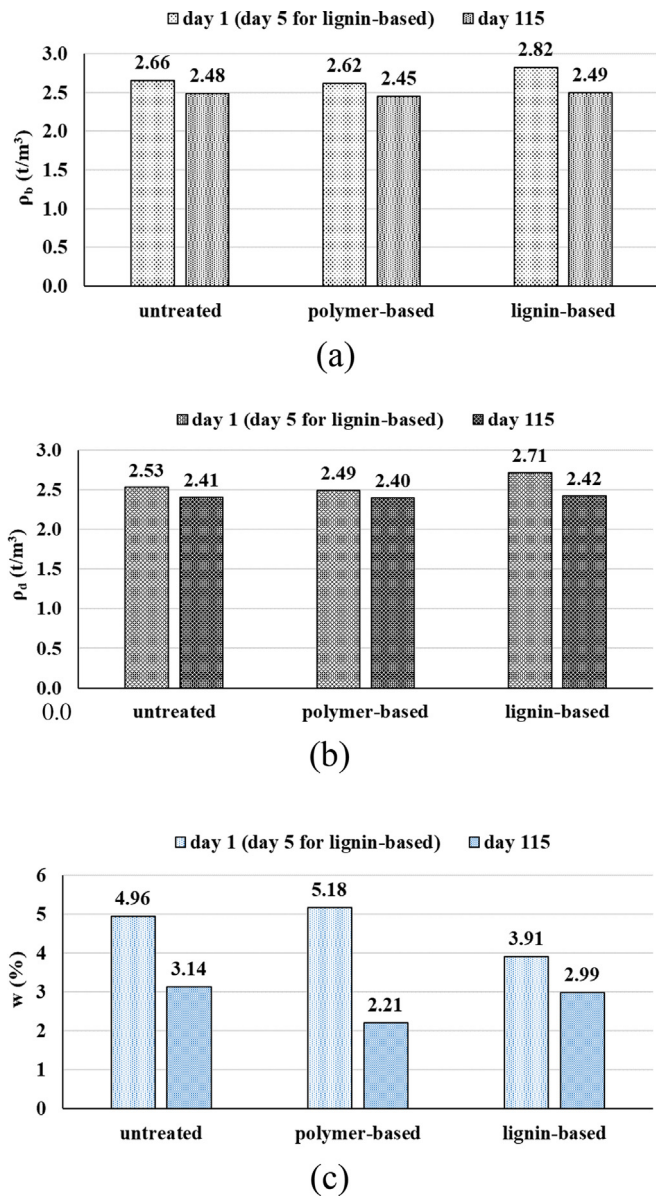
Fig. 10. Bulk density (a), dry density (b) and water content (c) for materials tested in the field after construction and after 115 days.

performance was related to the quantity of silicate minerals on the rocks surface: notwithstanding the reduced silica contents in gabbro (different from materials M2 and M3), this stabilizing agent

significantly enhanced the mechanical properties of material M4. The resilient modulus of the specimens newly tested in May 2019 is displayed in Fig. 8a with dashed lines. Fig. 8b shows the data points and the corresponding regression curves for M4 2019 and M4-L 2019. These results showed that the performance of the materials treated with both organosilane and lignosulfonate improved; on the other hand, the resilient modulus of untreated specimens slightly decreased.

In addition to stiffness, the additives entailed beneficial effects also regarding the permanent strain rates. Fig. 9 depicts the mobilized angle of friction φ_{mob} and the angle of friction at incremental failure φ_{max} linked to the boundary limits of strain rate adopted between shakedown behaviours given in Table 1; the additive application enhanced both the angles. The resistance to permanent deformation of the stabilized specimens slightly increased from May 2018 (Fig. 9a) to May 2019 (Fig. 9b).

A simple elastic analysis using the procedure described in example 2.4 of Huang's book [40] is performed considering the elastic moduli obtained in May 2019 referring to three scenarios: a layer entirely composed by untreated, organosilane-treated or lignosulfonate-treated aggregates, respectively. The analysis shows that resilient deflections can be expected to reduce from 0.22 mm to 0.13 mm with polymer-based treatment and to 0.10 mm with lignin-based treatment buttressing the beneficial effect engendered by the additives. Thinner layers of treated aggregates might be used to achieve the same deflection related to untreated aggregates.

Field test

The in situ density was assessed with the excavation method [13], two areas for each location were investigated and average values are presented; Fig. 10a displays the bulk density, Fig. 10b displays the dry density. The area treated with lignin-based additive had the highest value, this could be partly due to the fact that the lignosulfonate density (approximately 0.05 t/m³) was included. The water content was assessed after construction and after 115 days (Fig. 10c). Water contents were initially much higher than in the samples tested in the laboratory. The quantity of the additive used for location L2 was significantly higher than in the other two locations L0 and L1 (Table 2); therefore, location L2 was clearly oversaturated after construction and the first water content measurements were accomplished after 120 h. A similar issue took place during the preparation of RLTT samples in May 2018, as the specimens treated with lignin-based additive were oversaturated and needed a longer curing time compared to the specimens treated with polymer-based additive: as an input for further research, lower water percentages may be tested for samples stabilized with lignosulfonate.

Fig. 11 displays the appearance of the surfaces after 50 days; all the pictures were taken with the same zoom. Compared to the untreated location L0 (Fig. 11a), both the polymer-based and the lignin-based additive promoted the formation of bonded layers at location L1
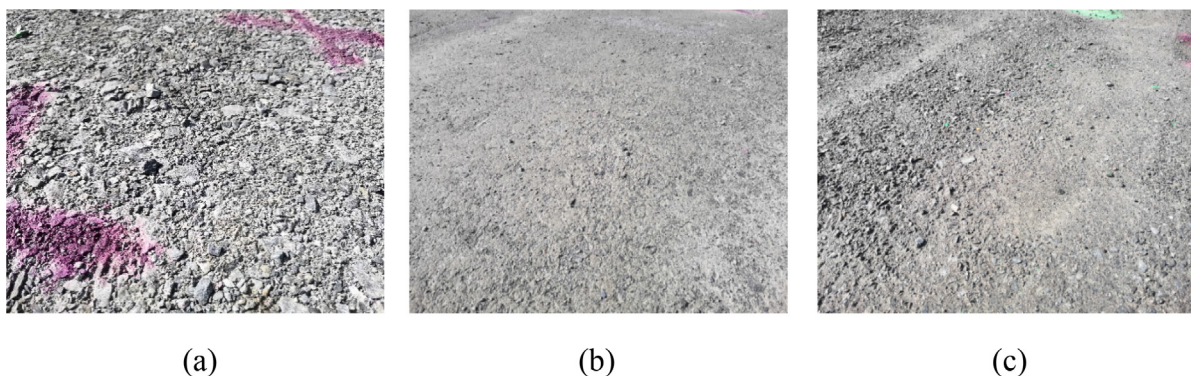

Fig. 11. Surface appearance after 50 days: untreated (a), with polymer-based additive (b) and with lignin-based additive (c).
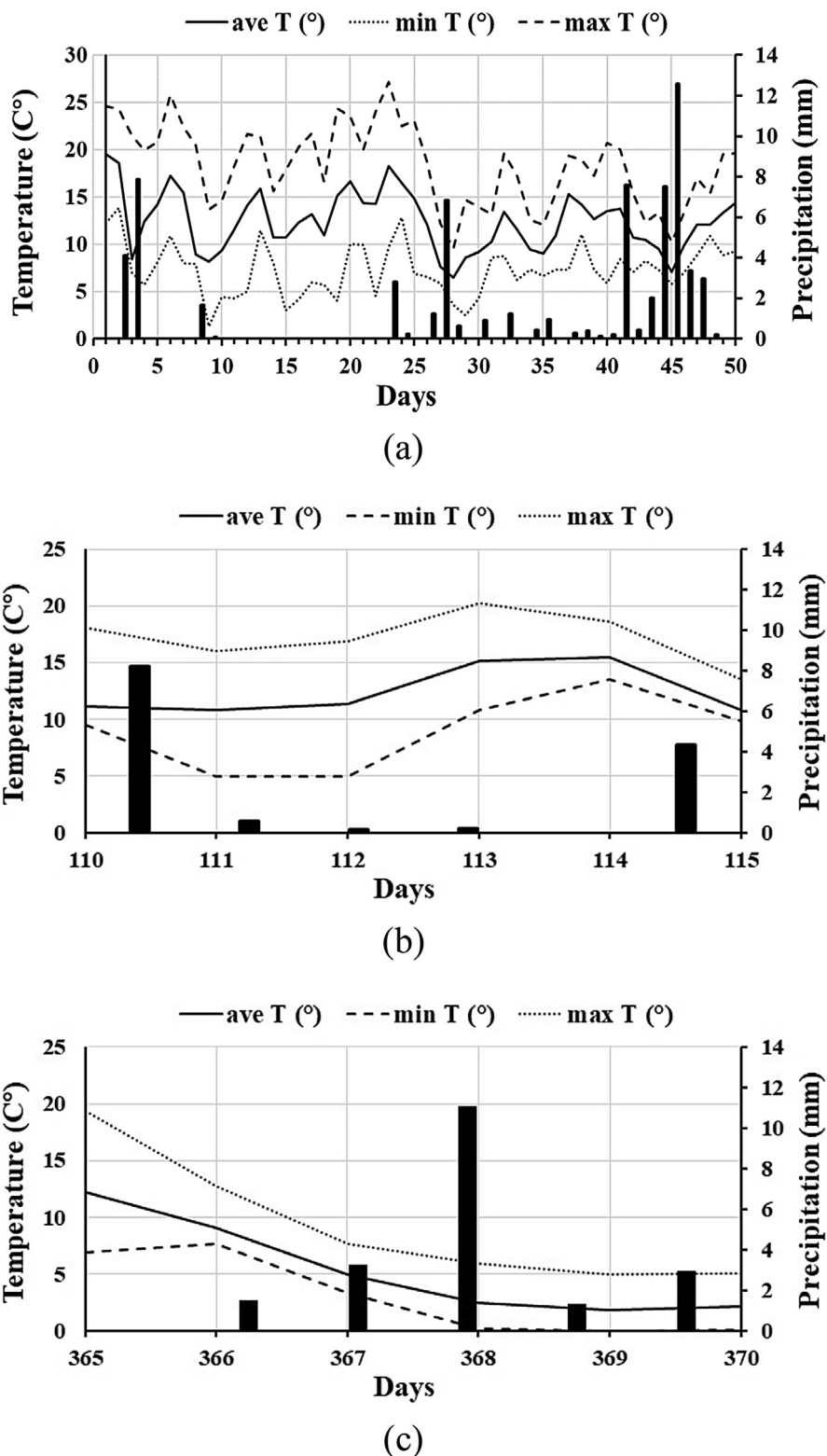
(a)

(b)

(c)

Fig. 12. Weather conditions in the field during the first 50 days after construction (a), from day 110 to day 115 (b), from day 365 to day 370 (c): average, minimum, maximum temperature and precipitation.

(Fig. 11b) and at location L2 (Fig. 11c), respectively.

Fig. 12a displays the weather conditions during the first 50 days after construction. The average temperature varied between 5 °C and 20 °C, rain started to take place approximately every day from day 24; this trend was exceptionally warm and dry in the Norwegian context [49]. After the initial 50 days, no LWD measurements were taken for a

period of 60 days. New LWD measurements were performed between day 110 and day 115 (September 2018); in this period, the mean values of average, minimum and maximum temperature were 12.5 °C, 8.9 °C and 17.2 °C, respectively, the cumulated precipitation was 13.4 mm (Fig. 12b). The last LWD measurements were accomplished between day 365 and day 370 (May 2019); in this period, the mean values of
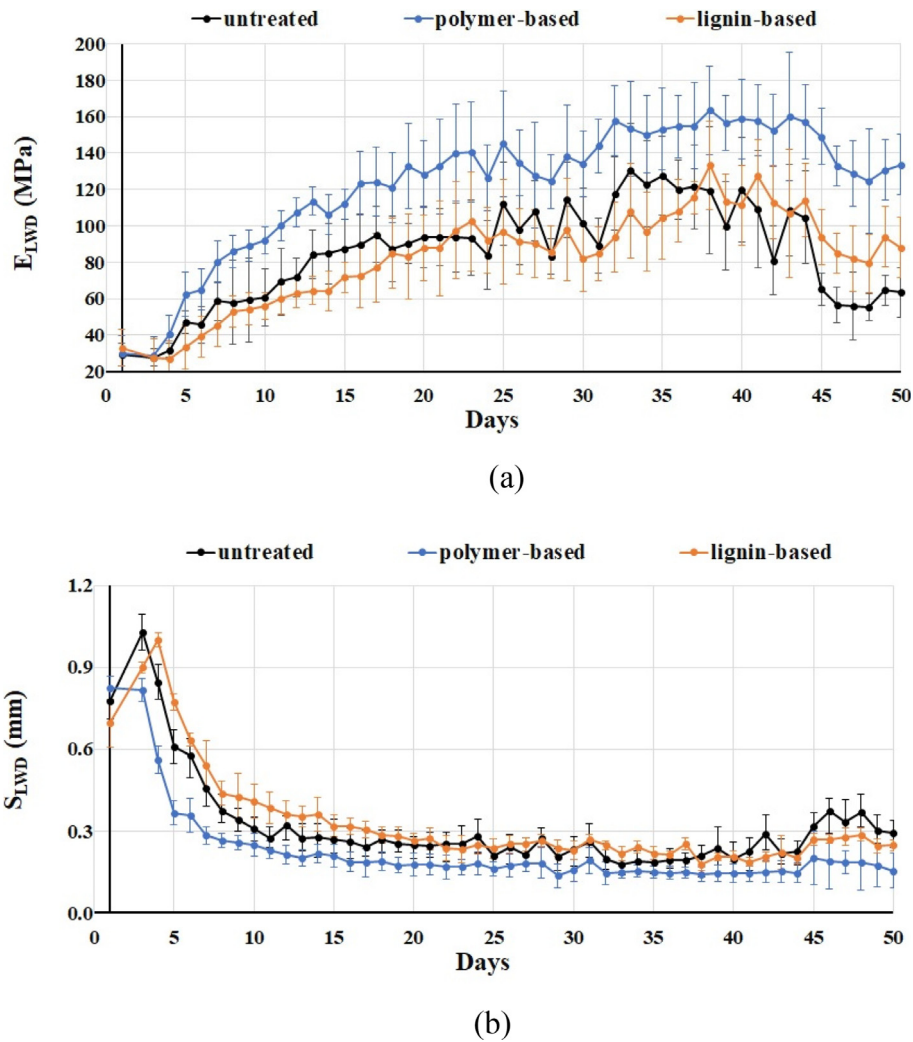
(a)

(b)

Fig. 13. LWD measurements results during the first 50 days after construction: elastic modulus E_{LWD} (a) and settlement S_{LWD} (b).
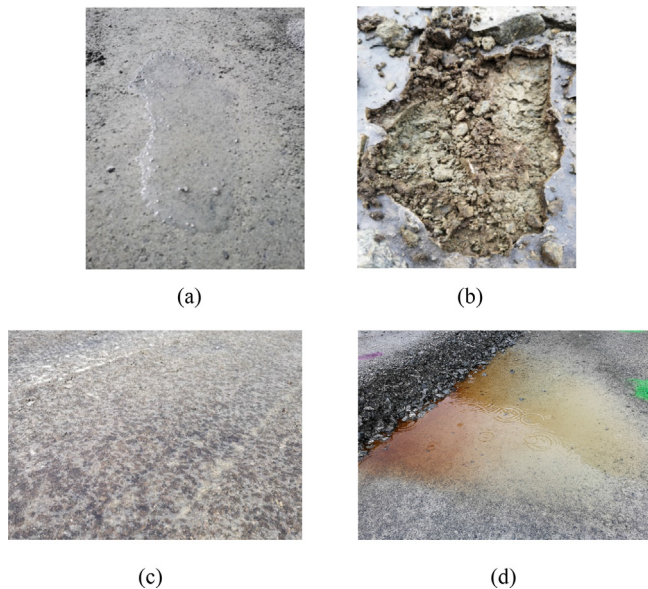

Fig. 14. Polymer-based additive: water poured on the surface (a); lignin-based additive: "crust" effect (b), "droplet" effect (c) and dissolution with water (d).

average, minimum and maximum temperature were 5.4 °C, 3.0 °C and 9.3 °C, respectively, the cumulated precipitation was 21.1 mm (Fig. 12c).

Light Weight Deflectometer

The LWD measurements were carried out daily during the first 50 days after construction, results are reported in Fig. 13: Fig. 13a shows the elastic modulus E_{LWD}, Fig. 13b displays the settlement S_{LWD}. Location L1 treated with organosilane had the highest E_{LWD} value (163.5 MPa) and the lowest S_{LWD} value (0.14 mm). The improvement of location L2 treated with lignosulfonate took place at a slower pace, and its performance became better than the untreated location L0 after 23 days; this may be due to having oversaturated location L2. This area reached 133.4 MPa as the highest E_{LWD} value and 0.18 as the lowest S_{LWD}. Both the treated locations L1 and L2 achieved their best performance values on day 38.

Location L1 became insensitive to water, as depicted in Fig. 14: the water, poured on the top of the layer on purpose, did not seem to penetrate (Fig. 14a). Some observations regarding location L2 can be made: while the lignosulfonate on the outermost part of the layer hardened forming a bonded "crust" with very few pores, the internal part still needed time to dry and attach to the material particles, as found by excavating approximately two centimeters below the surface (Fig. 14b). Most likely, this was the reason why it was possible to observe some lignosulfonate "droplets" reaching the surface during sunny days (Fig. 14c); moreover, this may also explain why the improvement
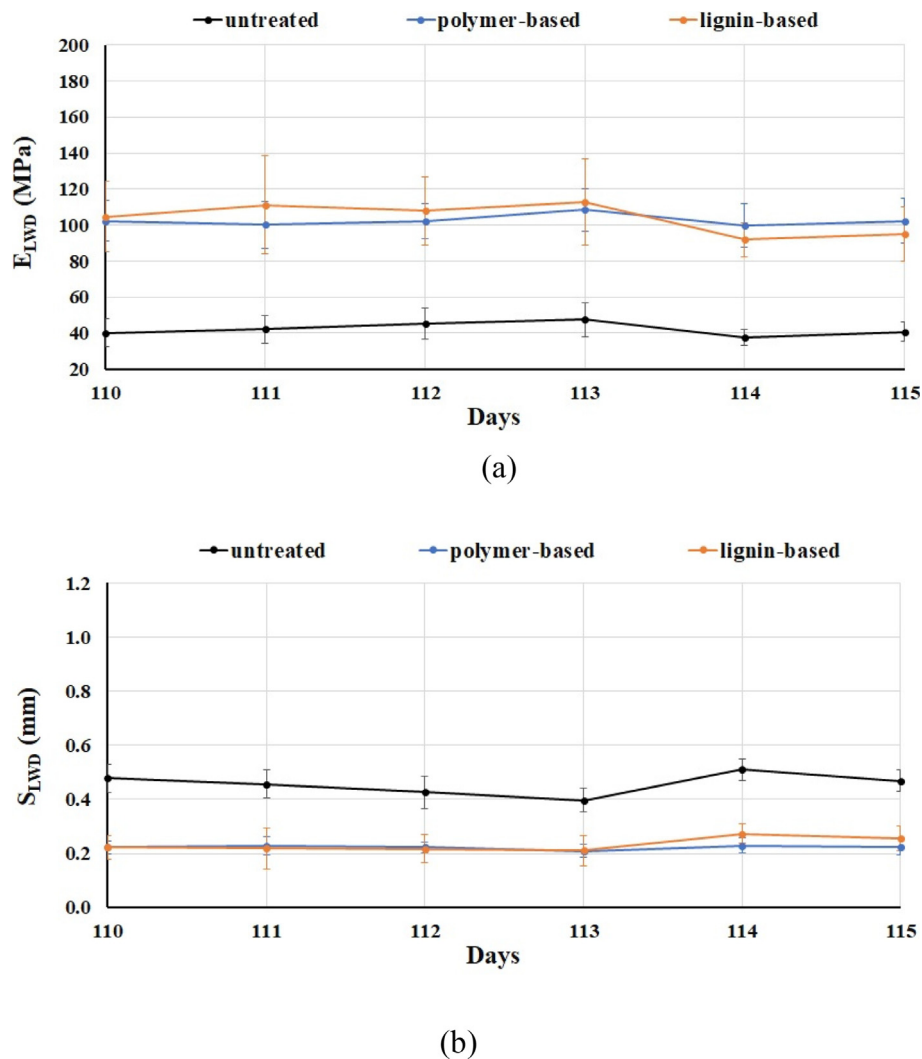
(a)

(b)

Fig. 15. LWD measurements results from day 110 to day 115: elastic modulus E_{LWD} (a) and settlement S_{LWD} (b).

of E_{LWD} values for location L2 took a longer time. The "crust" effect would probably have decreased if less water had been added, i.e. a higher concentrated solution of lignosulfonate; therefore, this may be an input for further research, both in the laboratory (as discussed previously) and in the field.

Lignosulfonate is water-soluble and partly dissolves in case of precipitation (Fig. 14d); therefore, the LWD results were affected by the rain, which took place almost every day after day 24. In addition, the untreated location L0 was the most vulnerable to water because there were meaningful changes in E_{LWD} and S_{LWD} values from day to day. On the other hand, even if the locations were not graded to have a cross profile to lead the water away, the changes due to precipitation for location L1 and L2 were smaller. During day 50 the E_{LWD} values were 63.5 MPa for location L0, 133.7 MPa (2.1 times E_{LWD} at L0) for location L1 and 88.1 MPa for location 2 (1.4 times E_{LWD} at L0).

Fig. 15 displays the LWD measurements performed from day 110 to day 115 after construction. The results showed that both the E_{LWD} values of the treated locations L1 and L2 were consistently higher than the E_{LWD} value of the untreated location L0 (Fig. 15a), similar considerations were valid also for settlement S_{LWD} (Fig. 15b). The values measured during this 5-day period were smaller than the maximum values obtained during the first 50 days. A plausible reason for this may be connected to the precipitation, which was more significant: during the first 50-day period the total cumulated precipitation was 66.0 mm, during the following 60-day period the value was 199.9 mm.

Fig. 16 displays the LWD measurements accomplished from day 365 to day 370, namely after one year from the construction. The results showed that the treated locations L1 and L2 continued to perform much better than the untreated location L0, even if a slight decrease in their values was registered compared to the previous monitored interval from day 110 to day 115. Differently from the increase in resilient modulus assessed in the laboratory as discussed in Section 'Repeated load triaxial test', there was no corresponding increment in the elastic modulus measured in the field. This may be due to the different environmental conditions: the specimens in the laboratory were exposed to temperature variation only, while the three field locations were subject to precipitation as well.

Dynamic Cone Penetrometer

The DCP measurements followed a determined procedure: 7 sequences composed of 3 blows were performed, the depth from the layer surface was recorded at the end of each sequence, Fig. 17 shows the results. Each location comprised 15 measurement points, as previously described in Section 'Measurement procedures'. The outcomes referring to the untreated location L0 just referred to 4 sequences (i.e. 12 blows), because a higher number of blows was enough to reach the layer's bottom.

Considering the results related to day 115, there was a switch in the trend of penetration rate between the area containing organosilane and the area containing lignosulfonate: the latter was stiffer up to 5
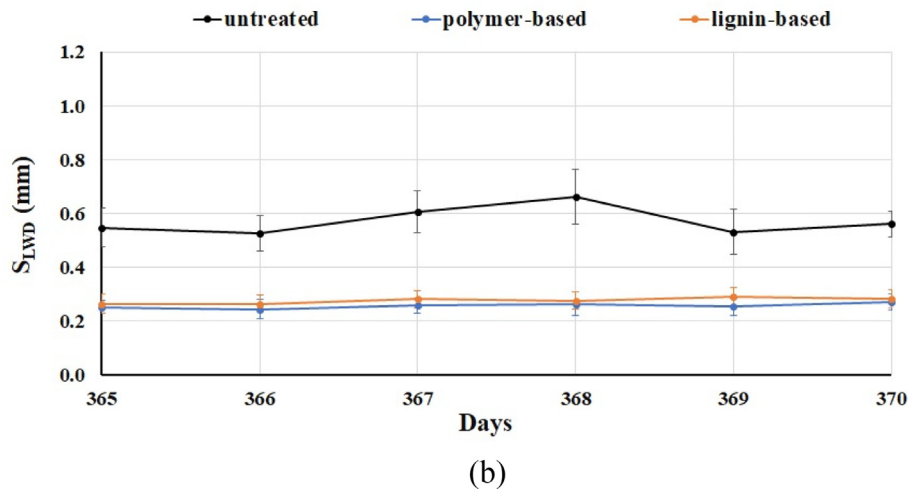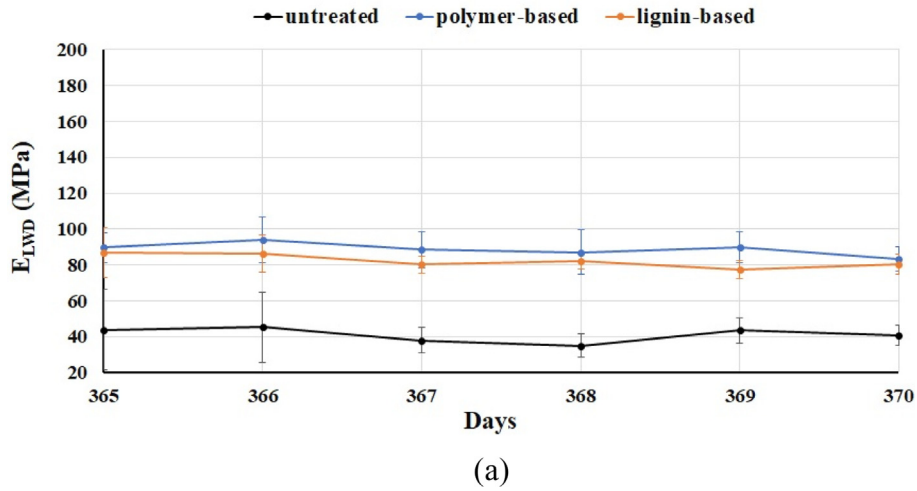
(a)

(b)

Fig. 16. LWD measurements results from day 365 to day 370: elastic modulus E_{LWD} (a) and settlement S_{LWD} (b).
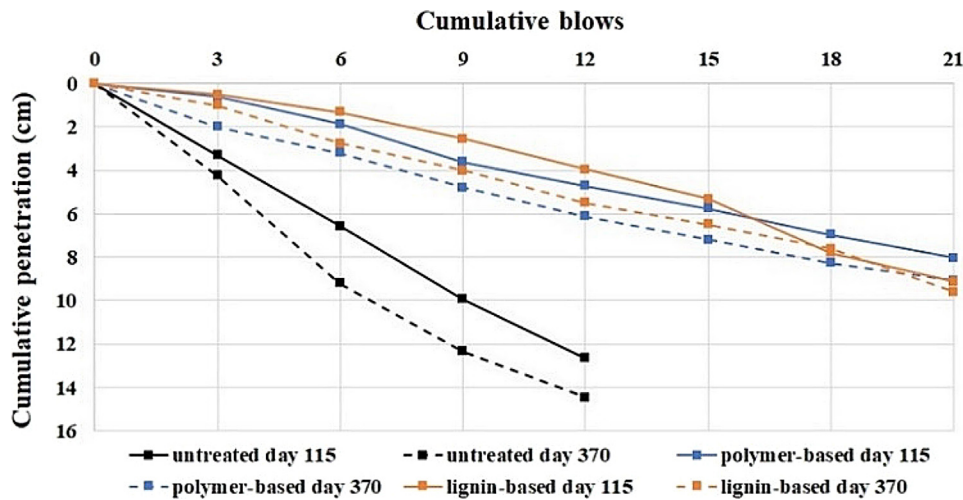

Fig. 17. DCP tests performed in day 115 and day 370 after construction.

sequences (i.e. 15 blows), which approximately corresponded to 5.5 cm. For a larger number of blows, namely for a major depth, the former achieved better results. This could be connected to the "crust" effect of the lignin-based treatment previously discussed in Section 'Light weight deflectometer'. Both the treated locations L1 and L2 performed better than the untreated location L0. The results obtained

for day 370 showed a general increase in the penetration values; nevertheless, the treated locations were still significantly stiffer than the untreated location.

Conclusions

The research examined two stabilizing additives that can improve the mechanical properties of crushed rocks to serve as construction materials, namely aggregates, in road unbound layers. One additive was based on organosilane, the other additive was based on lignosulfonate. Their effectiveness was assessed by means of laboratory and field tests; the time span covered by the investigations was one year. The application of the stabilizing agents can be particularly convenient for the aggregates not fulfilling the code requirements.

The laboratory tests comprised thin-section microscopy, X-Ray Diffractometry (XRD), X-Ray Fluorescence (XRF) for geological characterization and evaluation of silicates, and Repeated Load Triaxial Test (RLTT) for mechanical characterization.

The field tests were performed on three base road sections built according to real practice. One section was untreated, while the other two were treated with organosilane and lignosulfonate, respectively. The locations were exposed to climatic conditions only, no surface courses and no trafficking actions were applied. Light Weight Deflectometer (LWD) assessed the development of elastic modulus E_{LWD}; Dynamic Cone Penetrometer (DCP) measurements also contributed to the investigation. The samples investigated in the laboratory were exposed to temperature variation only (Fig. 7), while the field locations were subject to precipitation as well. The following conclusions can be drawn:

(1) The laboratory tests indicated that the investigated additives coat and bond the material particles closely together. The treated specimens had better mechanical properties than the untreated ones, both in terms of resilient modulus and resistance to permanent deformation.

(2) The field test showed that the organosilane additive had a rapid effect: LWD and DCP measurement operations proved that the treated materials performed better than the untreated materials. Furthermore, this additive apparently created an impermeable layer.

(3) The field test indicated that the lignosulfonate additive needed time to become effective; 23 days were necessary for the treated materials to exceed the untreated materials' performance. On the other hand, the amount of lignosulfonate and water used both in the laboratory and in the field led to oversaturation of the samples and "crust" formation in the field; therefore, as an input for further research, mixing proportions containing lower water percentages may be investigated.

(4) Lignosulfonate is water-soluble; the engineer needs to bear in mind this feature for road design and construction.

(5) The repetition of all the laboratory and field tests after one year highlighted the effectiveness of the stabilizing agents. Compared with the initial results, laboratory tests showed that the properties of the treated specimens were further enhanced; on the other hand, field tests showed that the properties of the treated locations slightly decreased.

(6) The tests accomplished in this research adopted aggregates that did fulfil standard code requirements. Based on the positive results obtained both in the laboratory and in the field, benefits may even be greater for poorer rock aggregates, which do not meet code specifications.

(7) On the whole the investigation demonstrated that both organosilane and lignosulfonate were effective solutions to enhance the properties of materials they were not especially designed for, namely crushed rocks used in road unbound layers.

CRediT authorship contribution statement

Diego Maria Barbieri: Conceptualization, Methodology, Software, Validation, Formal analysis, Investigation, Resources, Data curation, Writing - original draft, Visualization, Project administration. **Inge Hoff:** Conceptualization, Methodology, Validation, Investigation, Resources, Writing - review & editing, Visualization, Supervision, Project administration, Funding acquisition. **Mai Britt Engeness Mørk:** Investigation, Data curation, Writing - review & editing, Visualization, Supervision.

Declaration of Competing Interest

The authors declare that they have no known competing financial interests or personal relationships that could have appeared to influence the work reported in this paper.

Acknowledgments

References

[1] Alazigha DP, Indraratna B, Vinod JS. Mechanisms of stabilization of expansive soil with lignosulfonate admixture. Transp Geotech 2018;14:81–92. https://doi.org/10.1016/J.TRGEO.2017.11.001.

[2] ASTM International. Standard test method for use of the dynamic cone penetrometer in shallow pavement applications. USA; 2018.

[3] ASTM International. Standard test method for measuring deflections using a portable impulse plate load test device. USA; 2015.

[4] Barbieri DM, Hoff I, Mork H. Laboratory investigation on unbound materials used in a highway with premature damage. In: 10th Int. Conf. Bear. Capacit. Roads, Railw. Airfields; 2017.

[5] Barbieri DM, Hoff I, Mørk MBE. Mechanical assessment of crushed rocks derived from tunnelling operations. In: Cheng W-C, Yang J, Wang J, editors. 5th GeoChina Int. Conf. 2018 – Civ. Infrastructures Confronting Sev. Weather. Clim. Chang. From Fail. to Sustain., Springer; 2019a, p. 225–41. doi: https://doi.org/10.1007/978-3-319-95783-8_19.

[6] Barbieri DM, Hoff I, Mørk MBE. Innovative stabilization techniques for weak crushed rocks used in road unbound layers: a laboratory investigation. Transp Geotech 2019;18:132–41. https://doi.org/10.1016/j.trgeo.2018.12.002.

[7] Behnood A. Soil and clay stabilization with calcium- and non-calcium-based additives: a state-of-the-art review of challenges, approaches and techniques. Transp Geotech 2018;17:14–32. https://doi.org/10.1016/j.trgeo.2018.08.002.

[8] Berger A. Massedeponering. Beregning av kostnadsminimale tranportmønstre for planering av fjell- og jordmasser ved bygging av veier. Norwegian University of Science and Technology; 1978.

[9] Boussinesq J. Application des potentiels a l'etude de l'equilibre et du mouvement des Solids Elastiques. Paris: Gauthier-Villars; 1885.

[10] BS EN. Characterisation of waste. Leaching. Compliance test for leaching of granular waste materials and sludges. Part 2: one stage batch test at a liquid to solid ratio of 10 l/kg for materials with particle size below 4 mm (without or with size reduction); 2003.

[11] Burdin J, Monin N. The management of excavated materials from the Lyon-Turin rail link project. Geomech Und Tunnelbau 2009;2:652–62. https://doi.org/10.1002/geot.200900048.

[12] CEN. Geotechnical investigation and testing. Identification and classification of soil. Part 1: identification and description; 2018.

[13] CEN. Soil quality – Determination of dry bulk density; 2017.

[14] CEN. Tests for geometrical properties of aggregates. Part 1: determination of particle size distribution. Sieving method; 2012a.

[15] CEN. Tests for mechanical and physical properties of aggregates. Part 3: determination of particle shape – flakiness index; 2012b.

[16] CEN. Tests for mechanical and physical properties of aggregates. Part 1: determination of the resistance to wear (micro-Deval); 2011.

[17] CEN. Tests for mechanical and physical properties of aggregates. Part 2: methods for the determination of resistance to fragmentation; 2010.

[18] CEN. EN 13286-7 Cyclic load triaxial test for unbound mixtures. Belgium; 2004.

[19] CEN. EN 13286-4 Test methods for laboratory reference density and water content – Vibrating hammer. Belgium; 2003.

[20] Chen DH, Lin D, Liau P, Bilyeu J. A correlation between dynamic cone penetrometer values and pavement layer moduli. Geotech Test J 2005;28.

[21] Chen J, Hossain M, Latorella T. Use of falling weight deflectometer and dynamic cone penetrometer in pavement evaluation. Transp Res Rec 1999;1655:145–51. https://doi.org/10.3141/1655-19.

[22] Chen Q, Indraratna B, Carter J, Rujikiatkamjorn C. A theoretical and experimental study on the behaviour of lignosulfonate-treated sandy silt. Comput Geotech

2014;61:316–27. https://doi.org/10.1016/j.compgeo.2014.06.010.

[23] Daniels J, Hourani MS. Soil improvement with organo-silane. U.S.-China Work. Gr. Improv. Technol. 2009, Orlando; 2009. doi: doi.org/10.1061/41025(338)23.

[24] DD CEN/TS. Characterization of waste. Leaching behaviour tests. Up-flow percolation test (under specified conditions); 2006.

[25] Dongmo-Engeland B. GARAP, Influence of sample's height on the development of permanent deformation. Trondheim; 2005.

[26] Dunham KK. Coastal Highway Route E39 – Extreme crossings. Transp Res Procedia 2016;14:494–8. doi: 10.1016/j.trpro.2016.05.102.

[27] Elhakim AF, Elbaz K, Amer MI. The use of light weight deflectometer for in situ evaluation of sand degree of compaction. HBRC J 2014;10:298–307. https://doi.org/10.1016/j.hbrcj.2013.12.003.

[28] Erlingsson S, Rahman MS, Salour F. Characteristic of unbound granular materials and subgrades based on multi stage RLT testing. Transp Geotech 2017;13:28–42. https://doi.org/10.1016/j.trgeo.2017.08.009.

[29] Fleming P, Frost M, Lambert J. Review of lightweight deflectometer for routine in situ assessment of pavement material stiffness. Transp Res Rec J Transp Res Board 2007;2004:80–7. https://doi.org/10.3141/2004-09.

[30] Foroutan Mirhosseini A, Kavussi A, Tahami SA, Dessouky S. Characterizing temperature performance of bio-modified binders containing RAP binder. J Mater Civ Eng 2018;30:04018176. https://doi.org/10.1061/(asce)mt.1943-5533.0002373.

[31] Gomes Correia A, Winter MG, Puppala AJ. A review of sustainable approaches in transport infrastructure geotechnics. Transp Geotech 2016;7:21–8. https://doi.org/10.1016/j.trgeo.2016.03.003.

[32] Grenne T, Grammeltvedt G, Vokes FM. Ophiolites type sulphide deposits in the western Trondheim district, central Norwegian caledonides. Int Ophiolite Symp Cyprus: Cyprus Geol Surv Dep 1980:727–43.

[33] Haritonovs V, Tihonovs J, Smirnovs J. High modulus asphalt concrete with dolomite aggregates. Transp Res Procedia 2016;14:3485–92. https://doi.org/10.1016/j.trpro.2016.05.314.

[34] Hicks RG, Monismith CL. Factors influencing the resilient properties of granular materials. Highw Res Rec 1971:15–31.

[35] HMP-LFG. The light drop weight tester. Magdeburg prufgeratebau GmbH 2018 < https://www.hmp-online.com/en/ > [accessed September 10, 2018].

[36] HMP-LFG. HMP-LFG4 Instruction manual. Magdeburg; 2017.

[37] Hoff I. Dypstabilisering med fres - feltforsøk i Budalen. Trondheim; 2004.

[38] Hoff I, Bakløkk LJ, Aurstad J. Influence of laboratory compaction method on unbound granular materials. In: 6th Int. Symp. Pavements Unbound; 2003.

[39] Huang Y, Wang L. Experimental studies on nanomaterials for soil improvement: a review. Environ Earth Sci 2016;75:497. https://doi.org/10.1007/s12665-015-5118-8.

[40] Huang YH. Pavement Analysis and Design. Upper Saddle River; 2004.

[41] Jiang YJ, Fan LF. An investigation of mechanical behavior of cement-stabilized crushed rock material using different compaction methods. Constr Build Mater 2013;48:208–515. https://doi.org/10.1016/j.conbuildmat.2013.07.017.

[42] Kumar R, Adigopula VK, Guzzarlapudi SD. Stiffness-based quality control evaluation of modified subgrade soil using lightweight deflectometer. J Mater Civ Eng 2017;29. https://doi.org/10.1061/(ASCE)MT.1943-5533.0001958.

[43] Lekarp F, Isacsson U, Dawson A. State of the art. I: resilient response of unbound aggregates. J Transp Eng 2000a;126:66–75. doi: https://doi.org/10.1061/(ASCE)0733-947X(2000)126:1(66).

[44] Lekarp F, Isacsson U, Dawson A. State of the art. II: permanent strain response of unbound aggregates. J Transp Eng 2000b;126:76–83. doi: 10.1061/(ASCE)0733-947X(2000)126:1(76).

[45] Lieb R. Materials management at the Gotthard base tunnel – experience from 15 years of construction. Geomech Und Tunnelbau 2009;2:619–26. https://doi.org/10.1002/geot.200900032.

[46] Mooney MA, Miller P. Analysis of lightweight deflectometer test vased on in situ stress and strain response. J Geotech Geoenvironmental Eng 2009;135:199–208. https://doi.org/10.1061/(ASCE)1090-0241(2009) 135:2(199).

[47] Myre J. The use of cold bitumen stabilized base course mixes in Norway 2014:1–14.

[48] Neeb P-R. Byggeråstoff. Trondheim: Tapir; 1992.

[49] Norsk rikskringkasting AS. Varmerekord i Sør-Norge i mai 2018. < https://www.nrk.no/hordaland/varmerekord-i-sor-norge-i-mai-1.14054641 > [accessed July 9, 2019].

[50] Norwegian Meteorological Institute. eKlima 2019. < http://sharki.oslo.dnmi.no/portal/page?_pageid=73,39035,73_39049&_dad=portal&_schema=PORTAL > [accessed July 9, 2019].

[51] NPRA. Håndbok N200 vegbygging. Norway: Vegdirektoratet; 2018.

[52] NPRA. The E39 coastal highway route 2017a. < https://www.vegvesen.no/en/roads/Roads+and+bridges/Road+projects/e39coastalhighwayroute;jsessionid=99D143CB28F87A072777C744BBCA31E8?lang=nn > [accessed July 9, 2019].

[53] NPRA. Stabilisering av bærelag med DUSTEX, oppfølging av FOU rapport nr. 2008003393-1. 2017b.

[54] NPRA. Håndbok N200 vegbygging. Norway: Vegdirektoratet; 2014a.

[55] NPRA. Kalde bitumen- stabiliserte bærelag. Norway: Vegdirektoratet; 2014b.

[56] Paul DR, Robeson LM. Polymer nanotechnology: nanocomposites. Polymer (Guildf) 2008;49:3187–204. https://doi.org/10.1016/j.polymer.2008.04.017.

[57] Petkovic G. Recycling in Norwegian conditions. In: Nordal RS, Refsdal G, editors. 5th Int. Conf. Bear. Capacit. Roads Airfields, Trondheim: Tapir; 2005.

[58] Resch D, Lassnig K, Galler R, Ebner F. Tunnel excavation material – high value raw material. Geomech Und Tunnelbau 2009;2:612–8. https://doi.org/10.1002/geot.200900047.

[59] Riviera PP, Bellopede R, Marini P, Bassani M. Performance-based re-use of tunnel muck as granular material for subgrade and sub-base formation in road construction. Tunn Undergr Sp Technol 2014;40:160–73. https://doi.org/10.1016/j.tust.

2013.10.002.

[60] Roco MC. Broader societal issues of nanotechnology. J Nanoparticle Res 2003;5:181–9. https://doi.org/10.1023/A:1025548512438.

[61] Santoni RL, Tingle JS, Webster SL. Stabilization of silty sand with nontraditional additives. Transp Res Rec 2002:61–70.

[62] Shu B, Wu S, Dong L, Norambuena-Contreras J, Yang X, Li C, et al. Microfluidic synthesis of polymeric fibers containing rejuvenating agent for asphalt self-healing. Constr Build Mater 2019;219:176–83. https://doi.org/10.1016/j.conbuildmat.2019.05.178.

[63] Siekmeier J, Young D, Beberg D. Comparison of the dynamic cone penetrometer with other tests during subgrade and granular base characterization in Minnesota. In: Tayabji SD, Lukanen EO, editors. Nondestruct. Test. Pavements Backcalc. Modul. 3rd Vol., West Conshohocken, PA: American Society for Testing and Materials; 2000.

[64] Siripun K, Jitsangiam P, Nikraz H. Characterization analysis and design of hydrated cement treated crushed rock base as a road base material in Western Australia. Int J Pavement Res Technol 2010;10:39–47. https://doi.org/10.1080/10298430802342682.

[65] Sobolev K. Modern developments related to nanotechnology and nanoengineering of concrete. Front Struct Civ Eng 2016;10:131–41. https://doi.org/10.1007/s11709-016-0343-0.

[66] Sobolev K, Shah SP. Nanotechnology in construction. In: Sobolev K, Shah SP, editors. Proc. NICOM5, Springer; 2015, p. 509. doi: 10.1007/978-3-319-17088-6.

[67] Sun W, Wang L, Wang Y. Mechanical properties of rock materials with related to mineralogical characteristics and grain size through experimental investigation: a comprehensive review. Front Struct Civ Eng 2017;11:322–8. https://doi.org/10.1007/s11709-017-0387-9.

[68] Ta'negonbadi B, Noorzad R. Physical and geotechnical long-term properties of lignosulfonate-stabilized clay: an experimental investigation. Transp Geotech 2018;17:41–50. https://doi.org/10.1016/j.trgeo.2018.09.001.

[69] Teknologirådet. Teknologirådet | Norge 2030 arkiver 2012. < https://teknologiradet.no/category/norge-2030/ > [accessed July 9, 2019].

[70] Ugwu OO, Arop JB, Nwoji CU, Osadebe NN. Nanotechnology as a preventive engineering solution to highway infrastructure failures. J Constr Eng Manage 2013;139:987–93. https://doi.org/10.1061/(ASCE)CO.1943-7862.0000670.

[71] US National Weather Service. Precipitation measurements 2019. < https://www.weather.gov/abrfc/map > [accessed July 9, 2019].

[72] Uthus L, Tutumluer E, Horvli I, Hoff I. Influence of grain shape and texture on the deformation properties of unbound aggregates in pavements. Int J Pavements 2007;6.

[73] Vennapusa P, White D. Comparison of light weight deflectometer measurements for pavement foundation materials. Geotech Test J 2009;32.

[74] Wolff FC. Geologisk kart over Norge, berggrunnskart TRONDHEIM 1:250.000. Trondheim; 1976.

[75] Zhang T, Cai G, Liu S. Application of lignin-stabilized silty soil in highway subgrade: a macroscale laboratory study. J Mater Civ Eng 2018;30. https://doi.org/10.1061/(ASCE)MT.1943-5533.0002203.

[76] Zhang T, Cai G, Liu S. Application of lignin-based by-product stabilized silty soil in highway subgrade: a field investigation. J Clean Prod 2017;142:4243–57. https://doi.org/10.1016/j.jclepro.2016.12.002.

Diego Maria Barbieri is currently Postdoctoral Researcher at Norwegian University of Science and Technology, Norway, where he also recently completed his doctoral studies. He obtained the 2nd level postgraduate master and specialization diploma in railway engineering at La Sapienza University, Italy. He obtained his master and bachelor degree in Civil Engineering at University of Modena and Reggio Emilia, Italy. During this period, he had the opportunity to deepen his studies at Fuzhou University, PRC, as a visiting scholar. His research areas mainly comprise pavement engineering; he is particularly interested in investigating sustainable solutions for infrastructure construction.

Professor Dr. Inge Hoff has been doing research on materials for road, railway constructions and pavement design, especially use of unbound granular materials, for more than 20 years. His research interest is both on experimental work in laboratory or field and numerical modelling and design of roads and railways. Before starting to work as professor at NTNU nine years ago, he had been working at the independent research organization SINTEF.

Professor Dr. Mai Britt E. Mørk started as professor in geology at NTNU Department of Geology and Mineral Resources Engineering in 2003, now Department of Geoscience and Petroleum. She has geological background from University of Oslo and several years at SINTEF.